JOURNAL OF MATERIALS SCIENCE **34** (1999) 5549–5556

Effect of boron on phosphorus-induced temper embrittlement

S.-H. SONG, R. G. FAULKNER, P. E. J. FLEWITT*
Institute of Polymer Technology and Materials Engineering, Loughborough University, Loughborough, Leicestershire LE11 3TU, UK
**Bekerley Centre, Magnox Electric plc, Bekerley, Gloucestershire, GL13 9PB, UK*
E-mail: s.song@lboro.ac.uk

Combined equilibrium and non-equilibrium grain boundary segregation of solute atoms in dilute ternary alloys is modelled through consideration of site competition between two solutes. Model predictions are made for a low-alloy steel containing boron. The predicted results indicate that the kinetics of phosphorus segregation are dramatically facilitated by quenched-in vacancies, and the magnitude of the segregation, however, is substantially suppressed by the competition of boron with phosphorus for segregation sites, and in turn the phosphorus-induced embrittlement may be alleviated.

1. Introduction

Temper embrittlement is a common effect for low-alloy steels. This embrittlement refers to a loss in toughness that takes place when a low-alloy steel is heated in the range of approximately 350–600 °C or slowly cooled through this temperature range, leading to a tendency for intergranular brittle fracture and thus a shift in ductile-brittle transition temperature (DBTT) to higher temperatures. It is universally acknowledged that temper embrittlement is caused by grain boundary segregation of certain impurities like phosphorus. It is usually assumed [1–5] that the impurity segregation stems from an equilibrium segregation mechanism.

Most of the studies concerning phosphorus-induced temper embrittlement of low-alloy steels indicate [3, 6] that the greatest embrittlement effects emerge in the temperature range 500–550 °C. These studies are always done by the following heat treatment. The heat treatment steps of a sample are always quenching and toughening around 650 °C and then embrittling between 350 and 600 °C. In such an instance, the segregation of phosphorus is thermal equilibrium segregation, and the equilibrium segregation mechanism of temper embrittlement is in line with observations of the phosphorus segregation. In reality, most of the low-alloy structural steels, owing to the requirement of properties, cannot experience the toughening treatment above 600 °C. As a consequence, quenched-in vacancies should play an important part in the kinetics of temper embrittlement during tempering of commercial low-alloy steels directly after quenching, i.e., the temper embrittlement should be brought about by combined equilibrium and non-equilibrium segregation of phosphorus to grain boundaries. This viewpoint has been confirmed in an experimental study regarding the segregation behaviour of phosphorus in a low-alloy steel [7].

In view of the above considerations, we have established a combined equilibrium and non-equilibrium segregation model to explain phosphorus-induced temper embrittlement [8, 9]. The model is based upon an equilibrium segregation model and a non-equilibrium segregation model in dilute binary alloys.

A theoretical study on the effects of phosphorus and boron impurities on the energy and electronic properties of both an iron grain boundary and its corresponding intergranular fracture surface by the local density full potential augmented plane wave method [10] demonstrates that in contrast to the non-hybridised interaction between iron and phosphorus resulting in a grain boundary cohesion reduction, iron-boron hybridisation allows covalent bonding normal to the boundary to contribute to grain boundary cohesion. An experimental study on the effect of boron addition on the mechanical properties of a normalised 0.15C-0.22Si-1.25Mn steel [11] indicates that a minor addition of boron can decrease its impact transition temperature. Another similar study by Fukushima *et al.* [12] shows that a minor addition of boron in an Mn structural steel may increase its Charpy impact values under a quenched and tempered state. The experimental work by Chi *et al.* [13] reveals that 10 ppm boron addition in a 3Cr-Mo-V steel may effectively suppress its temper embrittlement due to boron segregation to grain boundaries. In addition, an investigation into the effects of boron on the phosphorus grain boundary segregation and intergranular fracture in high-purity Fe-0.2 wt %P-B alloys demonstrates [14] that an addition of 12.5 wt-ppm boron in the alloy may completely prevent its intergranular fracture induced by phosphorus segregation and thus decrease its ductile-brittle transition temperature (DBTT) by approximately 170 K when oil-quenched from 1073 K. Consequently, minor additions of boron

in low-alloy steels are beneficial to reducing their embrittlement.

There are two mechanisms for boron to enhance the grain boundary cohesion in iron [14], one of which is that the increased grain boundary cohesion is caused by boron itself as an inherent effect when it segregates at the boundary, the other is that boron suppresses phosphorus segregation by a site competition effect to alleviate the detrimental effect of phosphorus on the grain boundary cohesion. Some studies [14–16] have found the site competition effect between phosphorus and boron in Fe-B-P alloys.

In connection with the beneficial effect of boron addition on embrittlement of low-alloy steels, combined equilibrium and non-equilibrium grain boundary segregation of solute atoms in dilute ternary alloys has been detailed in this work on the basis of our previous work [8, 9, 17–20] through consideration of site competition in segregation between two solutes. To explain the beneficial effect of boron described above, model predictions have been made for boron-bearing low-alloy steels.

2. Model

2.1. Equilibrium segregation

Two solutes 1 and 2, in a ternary alloy, are considered here to compete with each other for sites at grain boundaries. The maximum equilibrium grain boundary concentrations of the two solutes in a dilute ternary alloy at a given temperature T, $C_\infty^{S1}(T)$ and $C_\infty^{S2}(T)$, in the approximation that all possible sites at grain boundaries are available for segregation of solute atoms, are given respectively by [3]

$$C_\infty^{S1}(T) = \frac{C_g^{S1}\exp(Q_{S1}/kT)}{1+C_g^{S1}\exp(Q_{S1}/kT)+C_g^{S2}\exp(Q_{S2}/kT)} \quad (1)$$

$$C_\infty^{S2}(T) = \frac{C_g^{S2}\exp(Q_{S2}/kT)}{1+C_g^{S1}\exp(Q_{S1}/kT)+C_g^{S2}\exp(Q_{S2}/kT)} \quad (2)$$

where C_g^{S1} and C_g^{S2} are the matrix concentrations of solutes 1 and 2, respectively; Q_{S1} and Q_{S2} are the segregation energies of solutes 1 and 2, respectively; and k is Boltzmann's constant.

When a sample is so quickly cooled from a high temperature T_i (quenching or solution-treatment temperature) to a lower temperature T_j that no mass transfer takes place in the sample during cooling, and then maintained at temperature T_j, the kinetics of equilibrium grain boundary segregation, derived by diffusional analysis, are given by [21]

$$\frac{C_{be}^{Sl}(t)-C_\infty^{Sl}(T_i)}{C_\infty^{Sl}(T_j)-C_\infty^{Sl}(T_i)} = 1-\exp\left(\frac{4D_s^{Sl}t}{\alpha_{e(Sl)}^2 d^2}\right)\mathrm{erfc}\left(\frac{2\sqrt{D_s^{Sl}t}}{\alpha_{e(Sl)d}}\right) \quad l=1,2 \quad (3)$$

where $C_{be}^{Sl}(t)$ is the grain boundary concentration of solute l after time t, D_s^{Sl} is the diffusion coefficient of solute l in the matrix, d is the thickness of the concentrated layer, and $\alpha_{e(Sl)}$ is the maximum equilibrium enrichment ratio of solute l, given by

$$\alpha_{e(Sl)} = C_\infty^{Sl}(T_j)/C_g^{Sl} \quad (4)$$

2.2. Non-equilibrium segregation

As detailed in Refs. [17–19], the non-equilibrium segregation mechanism relies on the formation of sufficient quantities of vacancy-solute complexes. Solute atoms, vacancies and their complexes are in equilibrium with each other at a given temperature. When a material which is properly held at a solution-treatment (or quenching) temperature is quickly cooled to a lower temperature, it will exhibit a loss of vacancies along grain boundaries, i.e., at vacancy sinks, whereby it achieves the equilibrium vacancy concentration corresponding to the lower temperature. The decrease in vacancy concentration brings about the dissociation of the complexes into vacancies and solute atoms. This in turn leads to a decrease in complex concentration in the neighbourhood of grain boundaries. Meanwhile, in regions remote from the grain boundary, where no other vacancy sinks are present, the vacancy concentration, which is nearly equal to the equilibrium vacancy concentration corresponding to the solution-treatment (or quenching) temperature, always remains. As a result, a complex concentration gradient appears between the grain boundary and the adjacent grains. The concentration gradient of the complexes causes their migration leading to an excess solute concentration in the vicinity of grain boundaries. It is obvious that the larger the supersaturation level of vacancies induced by solution-treatment (or quenching), the larger the segregation level of solute atoms resulting at the boundary.

Competition between two solutes for sites at the grain boundary will be dealt with by the following method. As described in Ref. [22], by the complex mechanism described above they first segregate to the grain boundary independently to get segregation levels C_{bn}^{S1} and C_{bn}^{S2}, and then distribute there in conformity to their binding energies with the grain boundary (equilibrium segregation energies). The competition effect could be evaluated by

$$C_{bn}^{S1^*} = C_{bn}^{S1}\left[\frac{C_g^{S1}\exp\left(\frac{Q_{S1}}{kT}\right)}{C_g^{S1}\exp\left(\frac{Q_{S1}}{kT}\right)+C_g^{S2}\exp\left(\frac{Q_{S2}}{kT}\right)}\right] \quad (5)$$

$$C_{bn}^{S2^*} = C_{bn}^{S2}\left[\frac{C_g^{S2}\exp\left(\frac{Q_{S2}}{kT}\right)}{C_g^{S1}\exp\left(\frac{Q_{S1}}{kT}\right)+C_g^{S2}\exp\left(\frac{Q_{S2}}{kT}\right)}\right] \quad (6)$$

where $C_{bn}^{S1^*}$ and $C_{bn}^{S2^*}$ are the final levels of non-equilibrium grain boundary segregation for solutes 1 and 2, respectively; and Q_{S1} and Q_{S2} are the binding energies of the grain boundary with solutes 1 and 2, respectively.

The above approach to describing site competition between two solutes is reasonable. Since non-equilibrium segregation is a kinetic process, the complexes

leading to this segregation may diffuse independently to the grain boundary. Similar to equilibrium segregation, the two solutes, however, need to re-distribute at the grain boundary in the light of their binding energies with the boundary.

Some experimental studies [20, 23] have shown that non-equilibrium grain boundary segregation can be classified into segregation and desegregation. When a sample is quickly cooled from a higher solution-treatment (or quenching) temperature to a lower temperature and then maintained at this lower temperature, there is a critical holding time at which the non-equilibrium segregation level will be maximum. If the holding time of the sample is shorter than the critical time, the diffusion of solute-vacancy complexes to the grain boundary will be dominant and the process is termed a segregation process; if the holding time is longer than the critical time, the process in which the diffusion of solute atoms from the boundary to the adjacent grains is dominant will also take place, termed a desegregation process.

A non-equilibrium grain boundary segregation model established in our previous work [19] is utilised to depict the process. The model states that when a sample is quickly cooled to a lower temperature T, from a higher solution-treatment (or quenching) one T_0 and then maintained at the lower temperature, the maximum concentration of non-equilibrium grain boundary segregation induced during holding at this lower temperature, $C_b^m(T)$, is given by

$$C_b^m(T) = C_g\left(\frac{E_b}{E_f^v}\right)\exp\left(\frac{E_b - E_f^v}{kT_0} - \frac{E_b - E_f^v}{kT}\right) \quad (7)$$

where C_g is the matrix concentration of the solute, E_f^v is the vacancy formation energy, k is Boltzmann's constant, and E_b is the vacancy-solute binding energy.

As stated in Ref. [17], the complex concentration is related to the matrix concentration of the solute and the exponential term containing the solute-point defect binding energy. As a consequence, in order to evaluate the effect of the competition for the complex formation between two solutes on the maximum concentration of non-equilibrium segregation in dilute ternary alloys, Equation 7 may be modified into

$$C_{b(Sl)}^m(T) = C_g^{Sl}\frac{E_{b(Sl)}}{E_f^I}\left[\frac{C_g^{Sl}\exp\left(\frac{E_{b(Sl)}}{kT_0}\right)}{\sum_l C_g^{Sl}\exp\left(\frac{E_{b(Sl)}}{kT_0}\right)}\right] \times \exp\left(\frac{E_{b(Sl)} - E_f^v}{kT_0} - \frac{E_{b(Sl)} - E_f^v}{kT}\right) \quad l = 1, 2 \quad (8)$$

where $C_{b(Sl)}^m$ is the maximum concentration of non-equilibrium segregation for solute l, $E_{b(SI)}$ is the solute l-vacancy binding energy, and C_g^{Sl} is the matrix concentration of solute l.

When a sample is so quickly cooled from a higher temperature T_i to a lower temperature T_j that no mass transfer occurs in the sample during cooling and held at temperature T_j, the non-equilibrium segregation kinetics, derived by means of Equation 8, are given by [19]

$$\frac{C_{bn}^{Sl}(t) - C_{b(Sl)}^m(T_i)}{C_{b(Sl)}^m(T_j) - C_{b(Sl)}^m(T_i)} = 1 - \exp\left(\frac{4D_c^{Sl}t}{\alpha_{n(Sl)}^2 d^2}\right)\mathrm{erfc}\left(\frac{2\sqrt{D_c^{Sl}t}}{\alpha_{n(Sl)}d}\right) \quad l = 1, 2 \quad (9)$$

where $C_{bn}^{Sl}(t)$ is the concentration of solute l at the concentrated layer as a function of holding time at temperature T_j, D_c^{Sl} is the diffusion coefficient of solute l-vacancy complexes in the matrix, $C_{b(Sl)}^m(T_j)$ is the maximum segregation level of solute l at temperature T_j, $C_{b(Sl)}^m(T_i)$ is the maximum segregation level of solute l at temperature T_i, i.e., the grain boundary concentration of segregant at the holding time $t = 0$ at temperature T_j, d is the thickness of the concentrated layer, and $\alpha_{n(Sl)} = C_{b(Sl)}^m(T_j)/C_g^{Sl}$.

Equation 9 is an isothermal kinetic relationship of non-equilibrium segregation for the segregation process. It describes the non-equilibrium segregation concentration of solute atoms at grain boundaries as a function of holding time at temperature T_j when the diffusion process of the complexes to the grain boundary is dominant. Using Equations 5, 6, 8 and 9, one may predict the non-equilibrium segregation level of solute l in the sample quenched from a higher temperature and then tempered at the tempering temperature.

It should be noted here that although Equation 9 is the same as Equation 3 in form, they are much different in nature. Equation 3 depicts the equilibrium grain boundary segregation induced by the solute equilibration at the boundary whereas Equation 9 describes the non-equilibrium grain boundary segregation induced by the complex diffusion to the boundary.

As mentioned above, a critical time, t_c, exists at a certain temperature. At a certain temperature when the critical time is longer than the effective time of solute diffusion corresponding to the cooling process, t_e, the process in which segregation is dominant takes place alone; nevertheless, when t_c is shorter than t_e, the process in which desegregation is dominant also occurs.

The critical time, t_c, is given by [17, 20]

$$t_c = \frac{B^2\ln(D_c/D_s)}{4\delta(D_c - D_s)} \quad (10)$$

where δ is a numerical constant, B is the grain size, D_c and D_s are the diffusion coefficients of solute-vacancy complexes and solute atoms, respectively.

As discussed elsewhere [20], any continuous cooling curve for a sample may be replaced by a corresponding stepped one, each step of which is set up by a horizontal segment with a vertical one so as to calculate an effective time at a given temperature for this cooling process so long as the step is small enough. The effective time formula of a stepped cooling curve consisting of n steps at temperature T is given by [20]

$$t_e = \sum_{i=1}^{n} t_i\exp\left(-\frac{E_m^c(T - T_i)}{kTT_i}\right) \quad (11)$$

where E_m^c is the migration energy for diffusion of the complexes in the matrix; t_i and T_i are the isothermal holding time and temperature at the ith step of the stepped curve, respectively.

When the effective time is longer than the critical time at temperature T_j, the process in which desegregation is dominant will take place. In such an instance, the grain boundary segregation level of solute atoms, $C_{bn}^{Sl}(t)$, is given by [19]

$$C_{bn}^{Sl}(t) = C_g^{Sl} + \frac{1}{2}\left[C_{bn}^{Sl}(t_c) - C_g^{Sl}\right] \left[\mathrm{erf}\left(\frac{d/2}{\left[4D_s^{Sl}(t-t_c)\right]^{1/2}}\right) - \mathrm{erf}\left(\frac{-d/2}{\left[4D_s^{Sl}(t-t_c)\right]^{1/2}}\right)\right] \quad l = 1, 2 \quad (12)$$

where t is the isothermal holding time at temperature T_j, and $t_c = t_c(T_j)$. Evidently, Equation 12 is merely concerned with desegregation. Hence the condition $t > t_c$ is necessary in the use of Equation 12.

It may be seen from Equation 10 that if $D_c < D_s$, there will be no non-equilibrium segregation effects. It should, however, be noted here that Equation 10 is applicable only when the maximum equilibrium segregation level is zero or at least very low. This means that only at high temperatures where the maximum equilibrium segregation level is quite low is Equation 10 applicable. In practice, tempering temperatures for low-alloy steels are usually lower than 600 °C. In this scenario, there could be quite a high maximum equilibrium segregation level for alloying or impurity elements such as boron and phosphorus. During tempering, there will be no net back-diffusion fluxes of solute atoms from the grain boundary to the adjacent grains until the maximum equilibrium segregation level is reached. As a consequence, even if $D_c < D_s$ there still will be non-equilibrium segregation effects before the maximum equilibrium segregation level is attained within a period required for a complex to diffuse from the grain centre to the boundary. For the same reason, before the maximum equilibrium segregation level is achieved the process in which desegregation is dominant cannot occur even if the effective time is longer than the critical time in the case where $D_c > D_s$. In this work, the grain boundary segregation level of solute atoms before reaching the maximum equilibrium segregation level will be calculated only, which is obviously consistent with the real situation.

Non-equilibrium segregation and thermal equilibrium segregation are two different processes in nature. Non-equilibrium segregation is a kinetic process whereas equilibrium segregation is a thermodynamic process. As a consequence, it may be envisaged that these two processes are independent of each other. In the calculations, the segregation level is taken to be the sum of the non-equilibrium and equilibrium segregation levels minus the matrix concentration.

2.3. Calculation of segregation level in the tempered sample

Equilibrium segregation occurs mainly during tempering and non-equilibrium segregation occurs mainly during both quenching and tempering. Calculation of segregation levels in the tempered sample has to be divided into two steps. The first step is calculation of the segregation level during quenching and the second step is during tempering. Details on the calculation may be seen elsewhere [8].

3. Results and discussion

In order to explore the effect of boron addition on temper embrittlement of low-alloy steels, the approach described in Section 2 is now applied to predictions of solute segregation in a low-alloy steel containing boron. Data used in the calculations are listed in Table I.

The diffusion coefficients are given by the following relations

$$D_c = D_{oc}\exp\left(-\frac{E_m^c}{kT}\right) \quad (13a)$$

$$D_s = D_{os}\exp\left(-\frac{E_s}{kT}\right) \quad (13b)$$

TABLE I Data used in the theoretical calculations

	In the ferrite region		In the austenite region	
	Phosphorus	Boron	Phosphorus	Boron
E_s (eV)	2.68 [24]	2.69 [25]	3.03 [25]	0.91 [25]
E_f^v (eV)	1.6 [26]	1.6 [26]	1.6 [26]	1.6 [26]
E_v^m (eV)	1.3 [27]	1.3 [27]	1.3 [27]	1.3 [27]
E_b (eV)	0.36 [28]	0.47 [28]	0.41 [28]	0.5 [28]
E_m^c (eV)	1.66 [7]	1.77 [7]	1.71 [7]	1.3
D_{os} (m^2/s)	7.12×10^{-3} [24]	100 [25]	2.83×10^{-3} [25]	2×10^{-7} [25]
D_{oc} (m^2/s)	1.7×10^{-5} [29, 30]	1.7×10^{-5} [29, 30]	1.7×10^{-5} [29, 30]	2×10^{-7}
C_g (at %)	0.072	Variable	0.072	Variable
Q (eV)	0.54 [31]	1.04 [14, 32]		
B (μm)	20	20	20	20
d (nm)	1	1	1	1

where D_c and D_s is the diffusion coefficients of vacancy-solute complexes and solute atoms in the matrix, respectively; D_{oc} and D_{os} are the pre-exponential constants for diffusion of the complexes and solute atoms, respectively; E_m^c is the migration energy for diffusion of the complexes; E_s is the activation energy for diffusion of solute atoms; T is the absolute temperature; and k is Boltzmann's constant.

It should be noted that boron is here thought of as a substitutional solute in α-Fe and as an interstitial solute in γ-Fe on the basis of diffusion data [33] and of relative solubilities, atom diameter, and interstitial hole sizes [34].

With provision for the fact that non-equilibrium segregation relies on the formation of sufficient quantities of solute-vacancy complexes and the movement of these complexes to defect sinks like grain boundaries, it is necessary to discuss mechanisms for migration of the complexes. The mechanisms for migration of substitutional solute-vacancy complexes have been discussed in detail elsewhere [7]. Here, the mechanisms for migration of interstitial solute-vacancy complexes will be described for fcc and bcc crystals.

The formation of a vacancy-interstitial solute complex can be imagined as the combination of an isolated vacancy and an isolated interstitial solute atom. As illustrated in Figs 1 and 2, The vacancy, marked as □, is situated at a nearest lattice site with respect to the solute atom, marked as ●, which is located at an octahedral interstitial position for either an fcc or bcc crystal.

Owing to the fact that migration of interstitial solute atoms is independent of that of vacancies, mechanisms for migration of the vacancy-interstitial solute complex and typical jump sequences are suggested as follows for the fcc and bcc crystals, respectively.

For an fcc crystal, there are two types of jump sequence to lead to long-range migration of the complex.

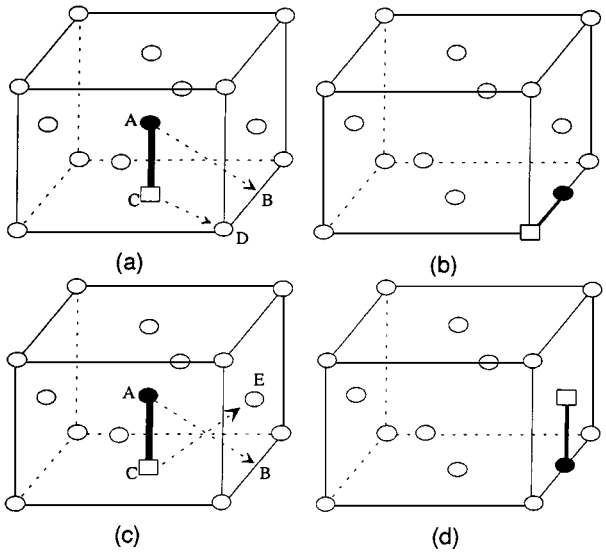

Figure 1 Schematic diagram showing (a) and (c) the migration processes of vacancy-interstitial solute complexes in fcc crystals with two different mechanisms; (b) and (d) the new positions of the complex after the jumps illustrated in (a) and (c), respectively (○: matrix atom; ●: solute atom; □: vacancy).

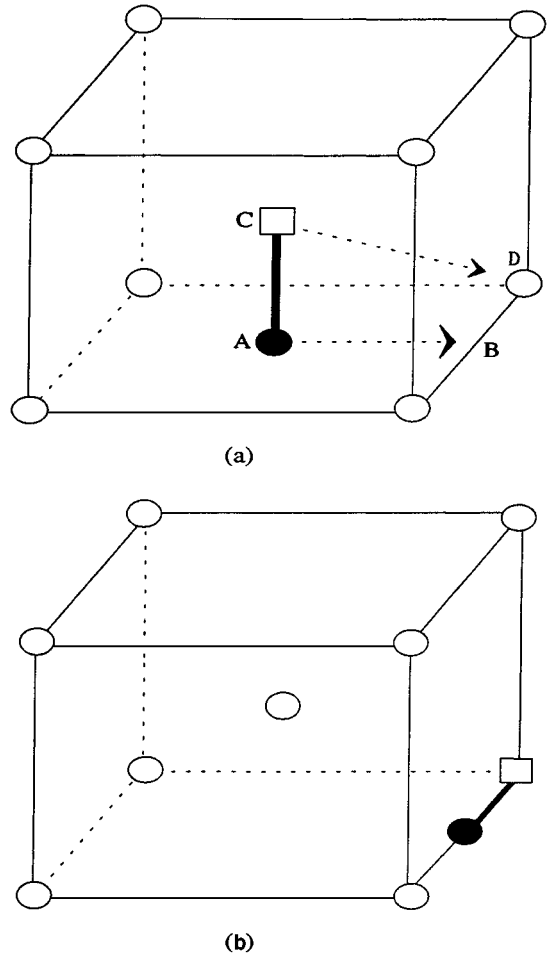

Figure 2 Schematic diagram showing (a) the migration process of vacancy-interstitial solute complexes in bcc crystals and (b) the new position of the complex after the jumps illustrated in (a) (○: matrix atom; ●: solute atom; □: vacancy).

Firstly, the solute atom involved in the complex, as illustrated in Fig. 1a, jumps from site A to site B and then the vacancy involved in the same complex jumps from site C to site D. After the jumps described above, the new position of the complex is shown in Fig. 1b. Secondly, the solute atom involved in the complex, as illustrated in Fig. 1c, jumps from site A to site B and then the vacancy involved in the same complex jumps from site C to site E. After the jumps described above, the new position of the complex is shown in Fig. 1d. Obviously, the migration of the complex does not need partial dissociation. As a result, the migration energy of the complex is approximately equal to the vacancy or solute-atom migration energy. The selection of the vacancy or solute atom migration energy is dependent on which has a higher value.

For a bcc crystal, first the solute atom involved in the complex, as illustrated in Fig. 2a, jumps from site A to site B and then the vacancy involved in the same complex jumps from site C to site D; or first the vacancy jumps from site C to site D and then the solute atom jumps from site A to site B. Evidently, although these two jump mechanisms both require the complex to dissociate partially and re-form and have the same effect, they need different energies. For the first mechanism,

the migration energy of the complex is approximately equal to the solute-atom migration energy plus the vacancy-solute binding energy or equal to the vacancy migration energy. The selection of the former or the latter is dependent on which is higher. For the second mechanism, the migration energy of the complex is approximately equal to the vacancy migration energy plus the vacancy-solute binding energy or equal to the solute-atom migration energy. The selection of the former or the latter is also dependent on which is higher. Since the migration energy of the vacancy is usually greater than that of the interstitial solute atom, the first migration mechanism of vacancy-interstitial solute complexes is more plausible than the second one.

It is assumed in the calculations that the heat-treatment procedures of a sample are:

(i) austenitizing at 1050 °C, 1250 °C, and 1300 °C, respectively, and oil-quenching;
(ii) tempering at 500 °C.

The analysis for segregation during quenching requires the quenching rate. The temperature as a function of cooling time, T, may be given approximately by [35]

$$T = (T_o - T_q)\exp(-\phi t) + T_q \qquad (14)$$

where T_o is the quenching temperature, T_q is the temperature of quenching medium, and ϕ is the cooling rate parameter, which is about 0.5 s^{-1} for oil-quenching for small samples [35].

Fig. 3 shows maximum equilibrium grain boundary segregation degrees of phosphorus versus tempering temperature with consideration of site competition between phosphorus and boron in a low-alloy steel doped with boron. Because of the competition of boron with phosphorus for segregation sites, the segregation of phosphorus is much suppressed, notably in the low and intermediate temperature ranges. In comparison with phosphorus segregation, there is not much change in boron segregation between with and without consideration of boron-phosphorus site competition (see Fig. 4). This means that the ability of site competition of phosphorus is much weaker than that of boron. As a consequence, boron should be a strong restrainer to grain boundary segregation of phosphorus.

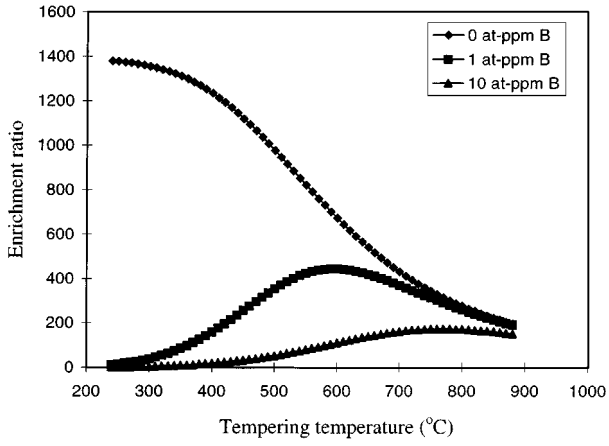

Figure 3 Maximum equilibrium enrichment ratios of phosphorus versus tempering temperature with consideration of site competition between phosphorus and boron in a low-alloy steel containing different quantities of boron.

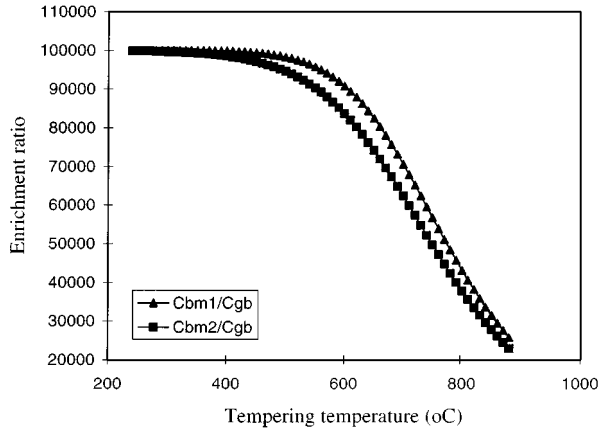

Figure 4 Maximum equilibrium enrichment ratios of boron versus tempering temperature without (Cbm1/Cgb) and with (Cbm2/Cgb) consideration of site competition between phosphorus and boron in a low-alloy steel doped with 10 at-ppm boron.

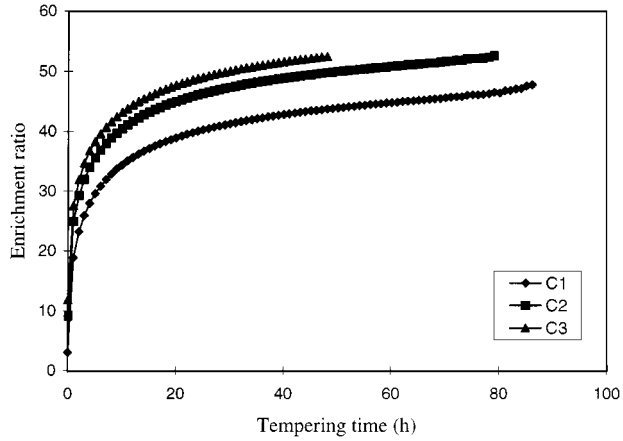

Figure 5 Predicted combined segregation of phosphorus versus tempering time with consideration of site competition between phosphorus and boron in a low-alloy steel doped with 10 at-ppm B oil-quenched from 1050 °C (C1), 1250 °C (C2), and 1300 °C (C3), respectively, and tempered at 500 °C (maximum equilibrium enrichment ratio is about 52).

Combined equilibrium and non-equilibrium segregation degrees of phosphorus in a low-alloy steel containing 10 at-ppm B quenched from different temperatures and tempered at 500 °C are illustrated in Fig. 5 as a function of tempering time with consideration of site competition between phosphorus and boron. Clearly, since the maximum equilibrium enrichment ratio is about 52 at 500 °C, the maximum segregation level of phosphorus may be achieved within approximately 79 and 48 h, respectively, for the 1250 °C- and 1300 °C-quenched samples. In addition, the segregation during quenching increases with increasing quenching temperature. This is because the concentration of quenched-in vacancies increases with increasing quenching temperature so that the non-equilibrium segregation of phosphorus increases during quenching and tempering.

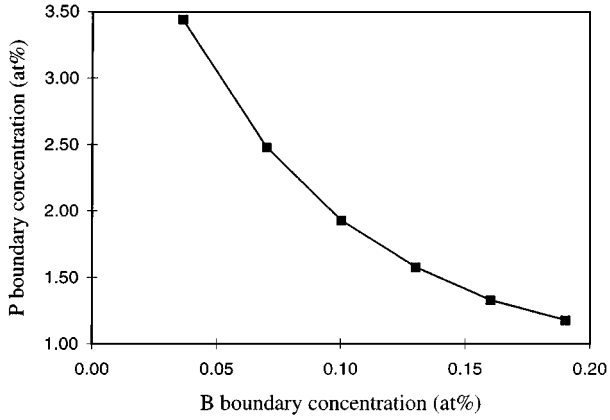

Figure 6 The predicted correlation between the grain boundary concentrations of phosphorus and boron in a low-alloy steel containing 0.072 at %P and 5, 10, 15, 20, 25, and 30 at-ppm B oil-quenched from 1050 °C and tempered at 500 °C for 10 h.

As described in Ref. [21], the times necessary to reach 1/2 and 9/10 of the maximum equilibrium segregation level, $t_{1/2}$ and $t_{9/10}$, are respectively

$$t_{1/2} = \frac{9\alpha_e^2 d^2}{64 D_s} \tag{15a}$$

$$t_{9/10} = 52 t_{1/2} \tag{15b}$$

where α_e is the maximum equilibrium enrichment ratio, D_s is the diffusion coefficient of segregant in the matrix, and d is the thickness of the concentrated layer.

Using Equation 15, one may obtain that the time required to reach 9/10 of the maximum equilibrium segregation level of phosphorus is about 219 h at 500 °C. As a result, the kinetics of phosphorus segregation are substantially facilitated by quenched-in vacancies. This means that the kinetics of temper embrittlement are dramatically promoted by the quenched-in vacancies and the magnitude of phosphorus segregation is considerably suppressed by the boron-phosphorus competition.

Fig. 6 represents the correlation between the grain boundary concentrations of phosphorus and boron in a low-alloy steel containing 0.072 at % P and 5, 10, 15, 20, 25, and 30 at-ppm B oil-quenched from 1050 °C and tempered at 500 °C for 10 h. Obviously, the segregation of phosphorus decreases with increasing boron segregation. This may be easily explained by the site-competition effect described in Section 2. Clearly, the predictions are generally consistent with the experimental observations described in the introduction section.

4. Summary

It has been confirmed that boron additions in low-alloy steels are beneficial to suppressing their temper embrittlement. In order to explain the beneficial effect of boron, combined equilibrium and non-equilibrium segregation of solute atoms in dilute ternary alloys has been modelled through consideration of site competition in grain boundary segregation between two solutes. Model predictions have been made for a boron-bearing low-alloy steel. The predictions demonstrate that the kinetics of phosphorus segregation are noticeably promoted by quenched-in vacancies, and the magnitude of the segregation, nevertheless, is considerably restrained by the competition of boron with phosphorus for segregation sites and for the formation of solute-vacancy complexes, and thus the detrimental effect of phosphorus on the grain boundary cohesion is suppressed. This is in agreement with the experimental results in regard to the effect of boron addition on embrittlement of low-alloy steels.

Acknowledgements

This work was financially supported by Magnox Electric and is published with the permission of the Director of Technology and Central Engineering of Magnox Electric.

References

1. W. STEVEN and K. BALAJIVA, *J. Iron Steel Inst.* **193** (1959) 141.
2. M. P. SEAH and C. LEA, *Surf. Sci.* **53** (1975) 272.
3. M. P. SEAH, *Acta Metall.* **25** (1977) 345.
4. C. L. BRIANT and S. K. BANERJI, *Int. Met. Rev.* **23**(4) (1978) 164.
5. I. OLEFJORD, *Int. Met. Rev.* **23**(4) (1978) 149.
6. R. A. MULFORD, C. T. MCMAHON JR., D. P. POPE and H. C. FENG, *Metall. Trans.* **7A** (1976) 1183.
7. R. G. FAULKNER, S.-H. SONG and P. E. J. FLEWITT, *Mater. Sci. Technol.* **12** (1996) 818.
8. S.-H. SONG and T.-D. XU, *J. Mater. Sci.* **29** (1994) 61.
9. S.-H. SONG, R. G. FAULKNER and H. JIANG, *J. Mater. Sci. Lett.* **13** (1994) 1007.
10. RUQIAN WU, A. J. FREEMAN and G. B. OLSON, *Science* **265** (1994) 376.
11. M. I. HAQ and N. IKRAM, *J. Mater. Sci.* **28** (1993) 5981.
12. M. FUKUSHIMA, S. SATO and Y. YOSHIDA, 9th International Congress on Heat Treatment and Surface Engineering and 5th French Open International Conference on Heat Treatment, Nice-Acropolis, France, 26–28 Sept. 1994. (PYC Edition, Cedex (France), 1994) pp. 465–473.
13. B.-H. CHI, T. FUJITA, K. SHIBATA and F. SHIMOMURA, *J. Iron Steel Inst. Jpn.* **78**(5) (1992) 798.
14. C. M. LIU, T. NAGOYA, K. ABIKO and H. KIMURA, *Metall. Trans.* **23A** (1992) 263.
15. T. MEGA, J. SHIMOMURA and E. YASUHARA, *Mater. Trans. JIM* **36** (1995) 1206.
16. T. MEGA, J. SHIMOMURA and K. SETO, *Mater. Trans. JIM* **37** (1996) 323.
17. R. G. FAULKNER, *J. Mater. Sci.* **16** (1981) 373.
18. *Idem., Acta Metall.* **35** (1987) 2905.
19. T.-D. XU and S.-H. SONG, *ibid.* **37** (1989) 2499.
20. S.-H. SONG, T.-D. XU and Z.-X. YUAN, *ibid.* **37** (1989) 319.
21. D. MCLEAN, "Grain Boundaries in Metals" (Oxford Univ. Press, London, 1957).
22. R. G. FAULKNER, S.-H. SONG, P. E. J. FLEWITT, M. VICTORIA and P. MARMY, *J. Nucl. Mater.* **255** (1998) 189.
23. T.-D. XU, S.-H. SONG, H.-Z. SHI, W. GUST and Z.-X. YUAN, *Acta Metall. Mater.* **39** (1991) 3119.
24. R. G. FAULKNER, S.-H. SONG and P. E. J. FLEWITT, *Metall. Mater. Trans.* **27A** (1996) 3381.
25. E. A. BRANDES and G. B. BROOK (eds.), "Smithells Metals Reference Book," 7th ed. (Butterworth-Heinemann, Oxford, 1992) pp. 13-70–13-102.
26. M. A. V. CHAPMAN and R. G. FAULKNER, *Acta Metall.* **31** (1983) 677.
27. M. KIRITANI, N. YOSHIDA, H. TAKATA and Y. MAEHARA, *J. Phys. Soc. Jpn* **38** (1975) 1677.

28. R. G. FAULKNER, S.-H. SONG and P. E. J. FLEWITT, *Mater. Sci. Technol.* **12** (1996) 904.
29. T. M. WILLIAMS, A. M. STONEHAM and D. R. HARRIES, *Metal Sci.* **10** (1976) 14.
30. S.-H. SONG and R. G. FAULKNER, *Defect and Diffusion Forum* **143-147** (1997) 149.
31. PH. DUMOULIN, M. GUTTMANN, M. FOUCAULT, M. PALMIER, M. WAYMAN and M. BISCONDI, *Met. Sci.* **14** (1980) 1.
32. M. HASHIMOTO, Y. ISHIDA, R. YAMAMOTO and M. DOYAMA, *Acta Metall.* **32** (1984) 1.
33. P. E. BUSBY and C. WELLS, *J. Metals* **6** (1954) 972.
34. C. C. MCBRIDE, J. W. SPRETANK and R. SPEISER, *Trans. ASM* **46** (1954) 499.
35. P. DOIG and P. E. J. FLEWITT, *Metall. Trans.* **18A** (1987) 399.

Received 18 June 1998
and accepted 16 April 1999